Environmental Research 180 (2020) 108900

Contents lists available at ScienceDirect

Environmental Research

journal homepage: www.elsevier.com/locate/envres

A possible relationship between telomere length and markers of neurodegeneration in rat brain after welding fume inhalation exposure

Mohammad Shoeb*, Gul M. Mustafa, Vamsi K. Kodali, Kelly Smith, Katherine A. Roach, Gregory Boyce, Terence Meighan, Jenny R. Roberts, Aaron Erdely, James M. Antonini

Health Effects Laboratory Division, National Institute for Occupational Safety and Health, Morgantown, WV 26505, USA

ARTICLE INFO

Keywords:
Welding fumes
Telomere
DNA damage
Trf1
Trf2

ABSTRACT

Inhalation of welding fume (WF) can result in the deposition of toxic metals, such as manganese (Mn), in the brain and may cause neurological changes in exposed workers. Alterations in telomere length are indicative of cellular aging and, possibly, neurodegeneration. Here, we investigated the effect of WF inhalation on telomere length and markers of neurodegeneration in whole brain tissue in rats. Male Fischer-344 (F-344) rats were exposed by inhalation to stainless steel WF (20 mg/m^3 x 3 h/d x 4 d/wk x 5 wk) or filtered air (control). Telomere length, DNA-methylation, gene expression of Trf1, Trf2, ATM, and APP, protein expression of p-Tau, α-synuclein, and presenilin 1 and 2 were assessed in whole brain tissue at 12 wk after WF exposure ended. Results suggest that WF inhalation increased telomere length without affecting telomerase in whole brain. Moreover, we observed that components of the shelterin complex, Trf1 and Trf2, play an important role in telomere end protection, and their regulation may be responsible for the increase in telomere length. In addition, expression of different neurodegeneration markers, such as p-Tau, presenilin 1-2 and α-synuclein proteins, were increased in brain tissue from the WF-exposed rats as compared to control. These findings suggest a possible correlation between epigenetic modifications, telomere length alteration, and neurodegeneration because of the presence of factors in serum after WF exposure that may cause extra-pulmonary effects as well as the translocation of potentially neurotoxic metals associated with WF to the central nervous system (CNS). Further studies are needed to investigate the brain region specificity and temporal response of these effects.

1. Introduction

A recent estimate indicated that 559,512 workers were employed as welders in the U.S. (https://datausa.io/profile/soc/514120/). However, millions of more workers worldwide perform welding as part of their work duties but are not considered full-time welders (Bureau of Labor Statistics, 2016). Welders are exposed to a fumes that are composed of a complex mixture of different potentially toxic metals, such as iron (Fe), manganese (Mn), copper (Cu), chromium (Cr), and nickel (Ni). Welding particulates are generally respirable and arranged as chain-like agglomerates of primary particles in the nanometer-size range with a mass mean aerodynamic diameter usually between 200 -500 nm (Antonini et al., 2013; Zeidler-Erdely et al., 2012). It has been well-documented that welding fume (WF) inhalation causes both acute (e.g., metal fume fever, transient lung function changes) and chronic (e.g., bronchitis, cancer) pulmonary effects (Antonini et al., 2003; Shoeb et al., 2017a). However, much less is known about the non-pulmonary effects of WF exposure, particularly the central nervous system (CNS).

There is growing evidence linking WF exposure and Mn accumulation in specific regions of the brain to neurological conditions, such as Parkinsonism (van der Mark et al., 2015; Li et al., 2004; Racette et al., 2012, 2017). WF exposure has been shown to cause alterations in Parkinson's disease-linked Park proteins, neuroinflammatory mediators, and glial cell activation in the brain of an animal model (Sriram et al., 2010). Also, Mn was been shown in the same study to accumulate rapidly and persist for extended periods of time in specific brain regions after WF exposure. The long post-exposure time point modeled a 'real-world' workplace scenario, whereas a latency between exposure and appearance of adverse neurological effects existed. Indeed, epidemiological studies have shown that welders may develop neurological dysfunction earlier than the general population, and such changes are often observed after the worker has left the occupation or been removed from exposure (Racette et al., 2012). Interestingly, a recent study of

* Corresponding author. Centers for Disease Control and Prevention, Health Effects Laboratory Division, National Institute for Occupational Safety and Health, 1095 Willowdale Road (Mailstop 2015) Morgantown, WV 26505, USA.
E-mail address: ywo7@cdc.gov (M. Shoeb).

https://doi.org/10.1016/j.envres.2019.108900
Received 21 August 2019; Received in revised form 23 October 2019; Accepted 5 November 2019
Available online 05 November 2019
0013-9351/ Published by Elsevier Inc.

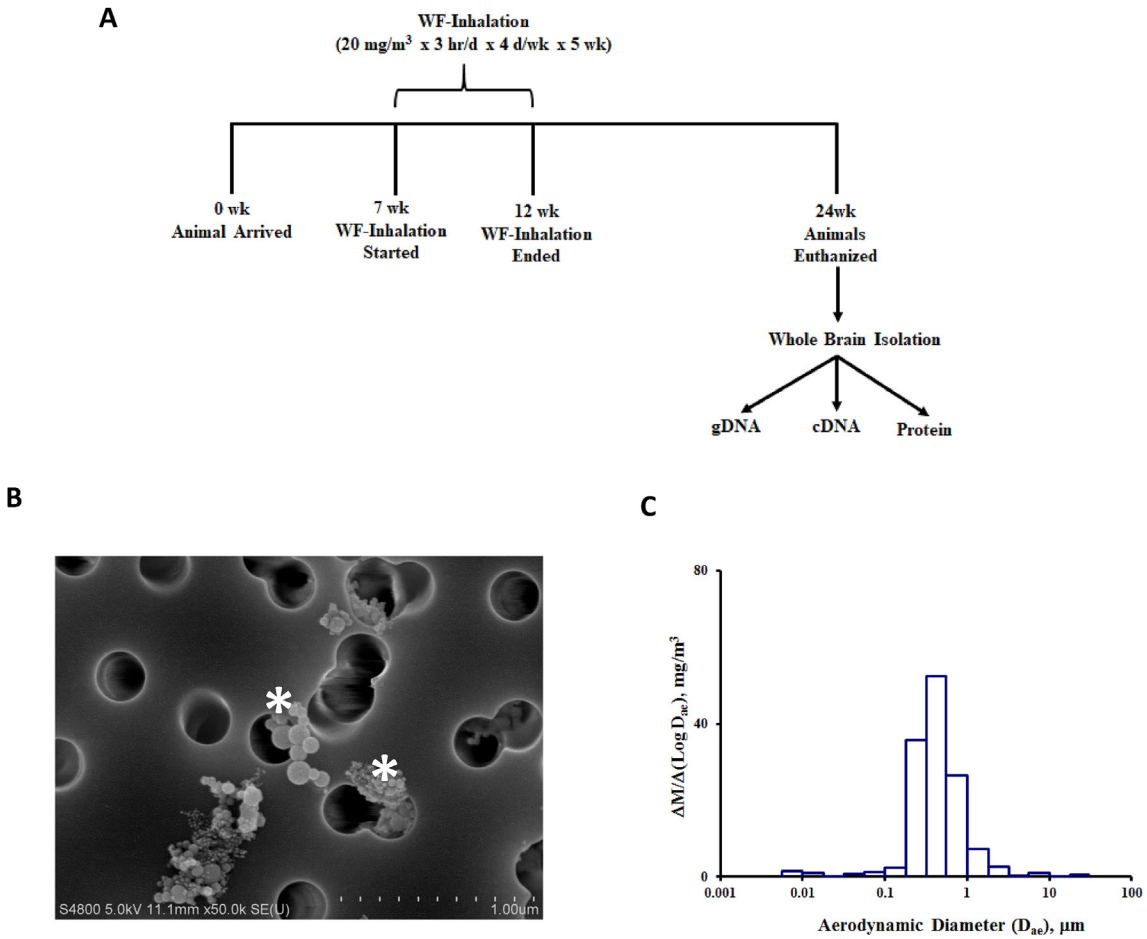

Fig. 1. (A) Experimental design for rats exposed by whole-body inhalation of aerosols generated during MMA-SS welding at concentration of 20 mg/m^3 x 3 h/d x 4 d/wk x 5 wk. Control animals were exposed to filtered air. At 12 wk after the WF exposure ended, rats were euthanized, brains were collected, and processed for isolation of gDNA, RNA or protein as described in methods. (B) SEM image of collected stainless steel WF. Note the welding particles were a combination of amorphous material (asterisks) and finer chain-like agglomerates composed of nanometer-sized, spherical primary particles. (C) Representative particle size distribution graph of WF that illustrates mass concentration, M, versus particle size, aerodynamic diameter; MMAD = 390 nm.

asymptomatic welders has indicated that Mn in WF, coupled with aging, may predispose workers exposed to WF more vulnerable to neurodegenerative conditions, such as Alzheimer's disease (Lee et al., 2019). As a neurodegenerative condition related to aging, Alzheimer's disease is characterized by Tau protein tangles, amyloid plaques, and loss of neuronal connections.

Telomeres are unique repetitive hexanucleotide sequences (TTAGGG) located at the end of chromosomes that preserve DNA integrity and genomic stability by protecting the ends of chromosomes from DNA damage and chromosomal end-to-end fusions. Normally, telomeres undergo shortening during mitosis. However, several factors may influence telomere length changes, such as aging, occupational exposure, cellular stressors, and lifestyle (Shoeb et al., 2017a, 2017b, 2019; Antonini et al., 2019). Telomeres protect the genome through different ways: (a) by preventing DNA polymerases replication of the entire genome leading to inappropriate processing of DNA repair enzymes because of a lack of RNA primers and (b) by preventing the switching from circular chromosomes to linear chromosomes. Protection of telomere and activation of the DNA damage response pathway (DDR) occurs through a protein complex, called shelterin, comprising telomere repeat factors 1 and 2 (Trf1 and Trf2), repressor/activator protein 1 (Rap1), Trf1-interacting protein 2 (Tin2), tripeptidyl peptidase 1 (Tpp1) and protection of telomere 1 (Pot1), called shelterin, which binds to the telomeres mainly through Trf1 and Trf2.

In the current study, we evaluated the effect of WF exposure on telomere length homeostasis and markers of neurodegeneration in rat brain. First, a functional *in vitro* assay was performed by which rat brain endothelial cells (EC) were exposed to the serum collected from the WF- and air-exposed animals to assess oxidative stress and a possible alteration in membrane permeability. Second, male F-344 rats were exposed by inhalation to stainless steel WF (20 mg/m^3 x 3 h/d x 4 d/wk x 5 wk) or filtered air (control). Rat brains were collected at 12 wk after WF exposure ended to assess the epigenetic changes (e.g., DNA methylation), alterations in telomere length, mRNA expression of Trf1 and Trf2, and effects on specific neurodegenerative markers, such amyloid precursor protein (APP), p-Tau, presenilin 1-2, and α-synuclein.

2. Materials and methods

2.1. In vitro ROS generation and change in membrane permeability

Rat primary brain microvascular endothelial cells (EC) were obtained from Cell Biologics (Cat# M1266; Chicago, IL) and were grown in DMEM containing 10% fetal bovine serum, 1% penicillin/streptomycin in a 95% air 5% CO_2-humidified atmosphere at 37 °C. Approximately 2 × 10^5 cells were seeded in chamber slides in a complete DMEM media and incubated overnight in a 95% air and 5% CO_2-humidified atmosphere at 37 °C. Cells were treated with 10% serum collected from WF- or air-exposed rats for 24 h. The cells were rinsed with phosphate-buffered saline (PBS), incubated with dihyrdroethidium (DHE; 2.5 µmol/l) 37 °C for 10–15 min, fixed in 10% formalin. Cells were washed in PBS twice and mounted with ProLong Gold. Random

images from each treatment group (n = 3) were taken using an Olympus AX70 upright microscope, and quantification was performed as previously described by (Shoeb et al., 2017a). Photomicroscopy of EC was obtained using a 40 × objective. The Millipore *in vitro* vascular permeability assay kit (ECM642) was used for evaluating the effects of serum collected from WF-exposed animals on EC permeability according to manufacturer instructions.

2.2. Animals

Male Fischer-344 rats (F-344/NHla CVF; Hilltop Lab Animals, Scottdale, PA) were received at 5 wk of age and were free of viral pathogens, parasites, mycoplasmas, Helicobacter, and CAR Bacillus, were used. The rats were acclimated after arrival until 12 wk of age and were provided HEPA-filtered air, irradiated standard Teklad 2918 diet and tap water ad libitum. All animal procedures used during the study were reviewed and approved by the CDC-Morgantown Institutional Animal Care and Use Committee. The animal facilities are specific pathogen-free, environmentally controlled, and accredited by the Association for AAALAC, International (Frederick, MD). All methods were performed in accordance with the relevant guidelines and regulations by CDC-NIOSH and AAALAC.

2.3. Welding fume exposure and characterization

A detailed description of the welding fume aerosol generator and inhalation exposure system was previously described (Antonini et al., 2006). The male F-344 rats were exposed by whole-body inhalation to aerosols generated during gas metal arc-stainless steel (GMA-SS) welding at a concentration of 20 mg/m^3 x 3 h/d x 4 d/wk x 5 wk (Fig. 1A). Control animals were exposed to filtered air. At 12 wk after WF exposure ended, rats in both groups (n = 6 air; n = 6 WF) were euthanized following an intraperitoneal injection of sodium pentobarbital euthanasia solution (> 100 mg/kg body weight; Fatal-Plus Solution, Vortech Pharmaceutical, Inc., Dearborn, MI). Whole brains were collected from all rats and processed as described in the following sections.

Analysis of elements present in the WF sample was performed using inductively coupled plasma-atomic emission spectroscopy (ICP-AES) using NIOSH method 7300 modified for microwave digestion (NIOSH, 1994). The metal composition of the GMA-SS WF sample was Fe (57%), Cr (20%), Mn (14%), Ni (9%), and Cu (0.2%) with trace amounts of Al, V, and Si. Welding samples were collected onto 47-mm Nuclepore polycarbonate filters (Whatman, Clinton, PA). The filters were mounted onto aluminum stubs with silver paste, and welding particles were imaged (Fig. 1B) using a Hitachi S4800 field emission scanning electron microscope (Bruker, Madison,WI). Particle size distribution (Fig. 1C) was determined in the exposure chamber in the breathing zone by using a MSP Model 110 Micro-Orifice Uniform Deposit Impactor (MOUDI) and a MSP Model 115 Nano-MOUDI (MSP Corporation, Shoreview, MN). The mass median aerodynamic diameter (MMAD) was determined to be 390 nm.

2.4. gDNA isolation and telomere length analysis

gDNA was extracted from the collected brain tissue and isolated using DNeasy Blood & Tissue Kit (Qiagen Sciences Inc., Germantown, MD). The DNA concentration was measured using a Nano-Drop 2000 spectrophotometer. Samples were diluted to a final concentration of 25 ng/1.5 µl to measure telomere length. Quantitative PCR (qPCR) was performed using the SYBR Select Master Mix (Life Technologies, Carlsbad, CA) with a step one plus real time PCR system (Applied Biosystems, Foster City, CA, USA). The parameters used were as follows: 95 °C for 10 min (enzyme activation), 95 °C for 15 s (denaturing), and 60 °C for 60 s (annealing), 60 cycles. Primers used were as follows: Tel rat-F 5′-GGT TTT TGA GGG TGA GGG TGA GGG TGA GGG TGA GGG t-3′, and Tel rat-R 5′-TCC CGA CTA TCC CTA TCC CTA TCC CTA TCC CTA TCC CTA- 3’; AT1 rat-F 5′-ACG TGT TCT CAG CAT CGA CCG CTA CC-3′ and AT1 rat-R 5′-AGA ATG ATA AGG AAA GGG AAC AAG AAG CCC-3’ (Invitrogen Corporation, Carlsbad, CA). The relative telomere length was measured by comparing the ratio of telomere repeat copy number (T as Tel1) and single gene copy number (S as AT1), expressed as telomere length (T/S) ratio. Each individual values obtained by qPCR were processed through formula $T/S = 2^{-\Delta CT}$, where ΔCT = CTtelomere – CTAT1. This ratio was then compared with the ratio of the reference DNA. Each DNA sample collected was measured in duplicate.

2.5. mRNA expression of Trf1, Trf2, ATM and APP

Relative mRNA levels were determined by qPCR. Total RNA was isolated from the brain tissue of the control (n = 6) and WF-exposed (n = 6) rats using a RNeasy Mini Kit (Qiagen Inc., Valencia, CA, USA), according to kit instructions. Briefly, 50–60 mg of brain tissue was homogenized in buffer RLT and one 5-mm stainless steel bead (Qiagen Inc, USA) using a tissue Lyser II (Qiagen Inc, USA). The tissue homogenate was centrifuged, and the RNA present in the supernatant was extracted and purified using RNeasy columns. RNA concentration was measured using the Nano-Drop 2000 spectrophotometer and reverse transcribed to synthesize cDNA from using random hexamers and Superscript III (Invitrogen, Carlsbad, CA, USA). cDNA was used for gene expression. Hypoxanthine-guanine phosphoribosyltranferase (HPRT) was used as the endogenous control. Gene expression was determined by standard 96-well technology using the StepOne Plus (Applied Biosystems, Carlsbad, CA) with pre-designed Assays-on-Demand TaqMan probes and primers including Trf1 and 2 (Rn01749291_m1, Rn01432601_m1), ATM (Rn01421973_m1), APP (Rn00570673_m1) (Thermo Fisher Scientific, Waltham, MA). In 96 well plates, cDNA was used for gene expression.

2.6. DNA methylation analysis

A DNA colorimetric quantification kit (Abcam, Cambridge, UK) was used to determine gDNA methylation according to manufacturer instructions and was previously described (Shoeb et al., 2017a). Briefly, binding buffer was added to each well then a negative control, positive control, or 400 ng of gDNA per reaction were added. The plate was incubated for 90 min, washed, and incubated with capture antibody for 60 min. The plate then was washed and incubated with detection antibody after which an enhancer solution was added. Finally, the plate was washed again, and developing solution was added followed by a stop solution. Absorbance was read at 450 nm.

2.7. Western blot analysis

Whole brain tissues were recovered from both treatment groups, separated, homogenized in tissue lysis buffer for Western blot analysis. The crude lysate was cleared by centrifugation at 12,000 × *g* for 10 min at 4 °C. An equal amount (10 µg) of protein lysate was separated using a 10–12% SDS-PAGE, and transferred to polyvinylidene difluoride membranes (Biorad, Hercules, CA). The membranes were incubated in blocking solution containing 5% w/v dried fat-free milk and 0.1% v/v Tween-20 in Tris-buffered saline. Subsequently, the membranes were incubated overnight with specific antibodies p-Tau (Ser416) (15013), presenilin 1 (5643), presenilin 2 (2192), α-synulein (2642) and GAPDH (2118) were obtained from Cell Signaling Inc. The blots were then washed, exposed to HRP-conjugated secondary antibodies for 1 h, and the antigen-antibody complex was detected by enhanced chemiluminescence (Pierce, Rockford, IL). The membranes were stripped and probed with antibodies against glyceraldehyde-3-phosphate dehydrogenase (GAPDH).

2.8. Capillary Western blot analysis

Capillary Western blot analysis (WES) was performed using the Protein-Simple Wes System. Briefly, whole-tissue lysate (brain) as prepared for Western blot analysis (above) was diluted with 10x sample buffer. Four parts of the diluted sample were mixed together with 1 part of 5x Fluorescent Master Mix and heated at 95 °C for 5 min. The Fluorescent Master Mix contained three fluorescent proteins that act as a 'ruler' to normalize the distance for each capillary because the molecular weight ladder is only on the first capillary, and each capillary is independent. After this denaturation step, the prepared samples, blocking reagent, primary antibodies Trf1 (ab66223) and Trf2 (ab69851), secondary antibodies and chemiluminescent substrate were dispensed into designated wells in an assay plate. A biotinylated ladder provided molecular weight standards for each assay.

2.9. Statistical analysis

Statistical differences between the WF and air groups were compared using a Student's t-test. Values represent means ± standard errors. Criterion of significance was set at $p < 0.05$.

3. Results and discussion

The goal of the present study was to use an animal model to assess the genotoxic and epigenetic effects of WF inhalation exposure on the brain. Neurotoxic metals (e.g., Mn) have been shown to accumulate in specific brain regions of workers (Lee et al., 2019; Sen et al., 2011) and laboratory animals (Sriram et al., 2010, 2012; Antonini et al., 2010) after WF exposure. In addition, we have observed elevated ROS generation in circulating peripheral blood mononuclear cells (PBMCs) at 24 h after exposure to stainless steel WF (Shoeb et al., 2017a). To further investigate the impact of WF inhalation in the circulation, a functional assay was performed by which rat brain EC were exposed to the serum collected from the stainless steel WF- and air-exposed animals for 24 h. Previously, it has been demonstrated that exposure of brain EC to serum recovered from MWCNT-exposed mice induced expression of adhesion molecules as well as disruption of blood brain barrier (BBB) permeability in a mouse model (Aragon et al., 2017). Furthermore, WF inhalation has been reported to cause 87% increased oxidative stress and 96% lipid peroxidation levels in PBMCs isolated from welders as compared to non-welders (du Plessis et al., 2010). In the current study, we observed a significant increase in ROS ($p = 0.05$) generation (Fig. 2A and B) and membrane permeability ($p = 0.01$) (Fig. 2C) in brain EC treated with serum collected from WF-exposed animal compared to air control animals. This suggested that factors present in serum after WF exposure can have extra-pulmonary effects in the central nervous system, influencing both BBB integrity and generation of potentially toxic ROS.

Compelling evidence suggests that telomere alteration is primarily due to increased oxidative stress and telomerase activity (Von Zglinicki, 2002; Hug and Lingner, 2006). Telomere length is regulated by telomeric DNA-binding proteins called shelterin proteins. Integral components of shelterin complex, Trf1, and Trf2, play an important role in telomere protection and regulation. Loss of Trf1 accelerates telomere length, indicating that Trf1 negatively regulates telomere length (Kishi et al., 2001). Trf1 regulates telomere length by affecting mitotic progression, whereas Trf2 prevents chromosomal fusion and mutations by maintaining the telomere t-loop structure (Spallarossa et al., 2009). Depletion of Trf2 could also result in the initiation of genomic instability and tumorigenesis (Nera et al., 2015). To investigate the effect of WF inhalation on telomere length homeostasis and Trf1/Trf2 dysregulation in the brain, rats were exposed to WF inhalation for 5 weeks, and the effects were examined 12 wk after WF exposure ended.

Our data showed that WF exposure resulted in changes in telomere length ($p = 0.01$) and DNA methylation, a marker of epigenetic alteration, compared to air control rat brain (Fig. 3A and H). However, we did not observe any changes in TERT mRNA expression in the WF-exposed group compared to the control group (Fig. 3B). Therefore, we reasoned that telomere lengthening after WF inhalation may not be due to telomerase activation. The telosome is comprised of six polypeptides and maintains the telomere length by recruiting telomerase and shielding telomeres from DNA damage response (DDR) (Mamdani et al., 2015). Telomere length is regulated by the telosome, and down-regulation, inhibition or deletion of Trf1 may cause elongated telomere length (van Steensel and de Lange, 1997; Chong et al., 1995). Our results revealed a significant decrease in Trf1 mRNA ($p = 0.05$) and protein expression (Fig. 3C and D), suggesting the involvement of Trf1 in telomere length elongation after WF inhalation.

In addition, telomeres prevent chromosomal end-to-end fusions by utilizing the restoration of double-strand DNA breaks. Repression of ATM kinase signaling pathway has been reported to be inhibited by Trf2 (Denchi and de Lange, 2007). Trf2 is located at double stranded telomeric DNA, and its overexpression has also been reported to negatively regulate telomere length (Smogorzewska et al., 2000; Ancelin et al., 2002). Ataxia-telangiectasia (A-T) is a rare autosomal genetic disease caused by mutations in the ATM gene, leading to neurodegeneration and other genomic dysfunctions (Shen et al., 2016). We observed significantly increased expression of ATM mRNA expression ($p = 0.02$) in the WF-exposed rat brains compared to air-exposed controls (Fig. 3G). Interestingly, decreased mRNA and protein expression of Trf2 gene was also observed in brain tissue of WF-exposed rats compared to control (Fig. 3E and F). These results suggest that neurotoxic metals present in WF or unknown circulatory factors that have accessed the CNS via a leaky BBB may be responsible for the effects on telomere length through a possible down-regulation of shelterin components Trf1 and Trf2.

Telomere shortening is a hallmark of aging of different organs due to limited cell division. Importantly, accelerated telomere shortening was observed in peripheral blood cells, however, elongated telomere length was reported in hippocampus of Alzheimer's brains of same patients compared to normal tissues (Thomas et al., 2008). Telomere elongation in these (AD) patients could possibly be due to continuous replication of dendate gyrus cells of the hippocampus (Kuhn et al., 1996; Eriksson et al., 1998). Early aging and accumulation of beta-amyloid protein are the characteristics of progressive neurodegeneration and related pathologies. The most common characteristic of neurodegenerative pathologies is the formation of protein aggregates, such as tau protein (p-Tau) aggregates and α-synuclein protein aggregates. Furthermore, β-amyloid expression has been observed in other neurodegenerative diseases, including PD and Lewy-body dementia (LBD) (Kurosinski et al., 2002). Previous studies have revealed an interaction between beta-amyloid and α-synuclein. Both β-amyloid and presenilin 1 deposition cause the aggregation of α-synuclein (Winslow et al., 2014; Compta et al., 2014). To explore how increased telomere length may affect the localization of APP, p-Tau, α-synuclein, presenilin 1 and 2 in rat brain after WF exposure, we analyzed expression of these specific neurodegenerative markers. Our results suggest an increased mRNA expression ($p = 0.01$) of APP, and protein expression of p-Tau, α-synuclein, presenilin 1 and 2 in brain tissue from the WF-exposed group compared to control (Fig. 4A and B).

These findings support a model for welders exposed to WF during their work duties potentially leading to persistent DNA damage, a dysfunctional shelterin complex (Trf1 and Trf2), and the eventual development of neurodegenerative diseases (Fig. 5). Collectively, our results suggest that WF inhalation may cause increased telomere length and expression of neurodegeneration markers in rat brain tissue through (Bureau of Labor Statistics, 2016): down-regulation of Trf1 and Trf2 (Antonini et al., 2013), activation of ATM-dependent DNA damage response machinery. Further, our data suggest that WF-mediated elongation of telomeres occurred without affecting telomerase function. We also present possible evidence that integral components of shelterin

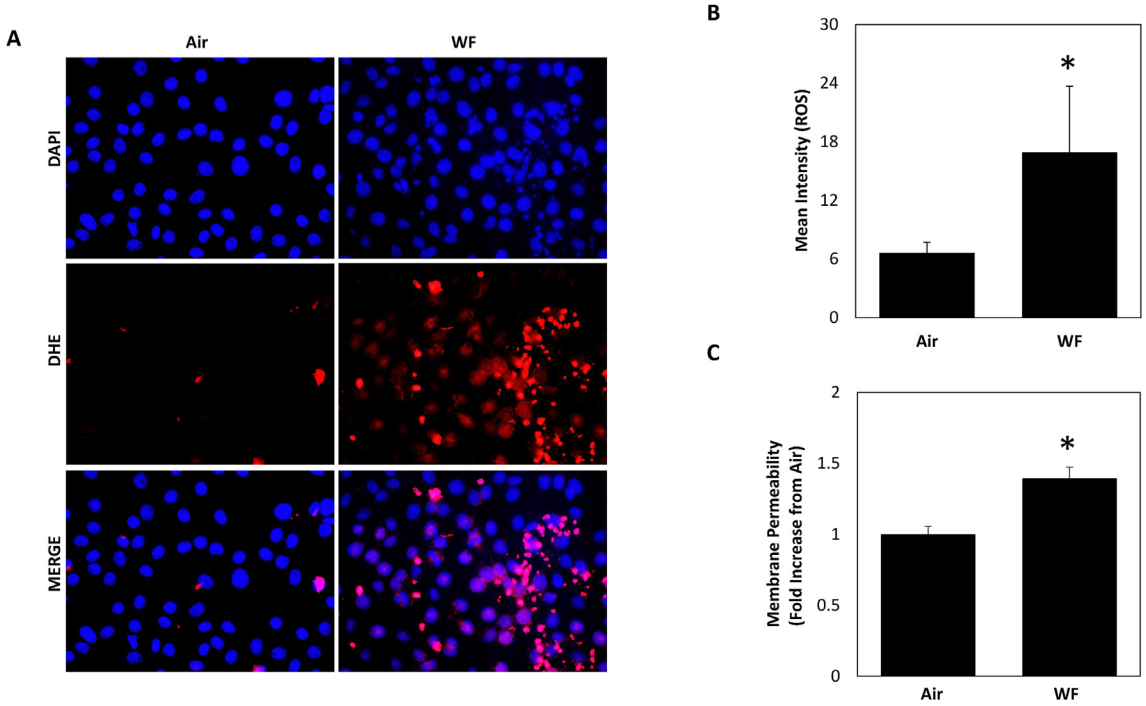

Fig. 2. (A–B) Reactive oxygen species generation (DHE; red fluorescence), quantification of reactive oxygen species-DHE response as measured by mean red fluorescence intensity; (C) level of membrane permeability in rats EC at 24 h after serum exposure recovered from WF-exposed animals. n #3; values are means ± standard error; *significantly different between air and WF groups, $p < 0.05$. (For interpretation of the references to color in this figure legend, the reader is referred to the Web version of this article.)

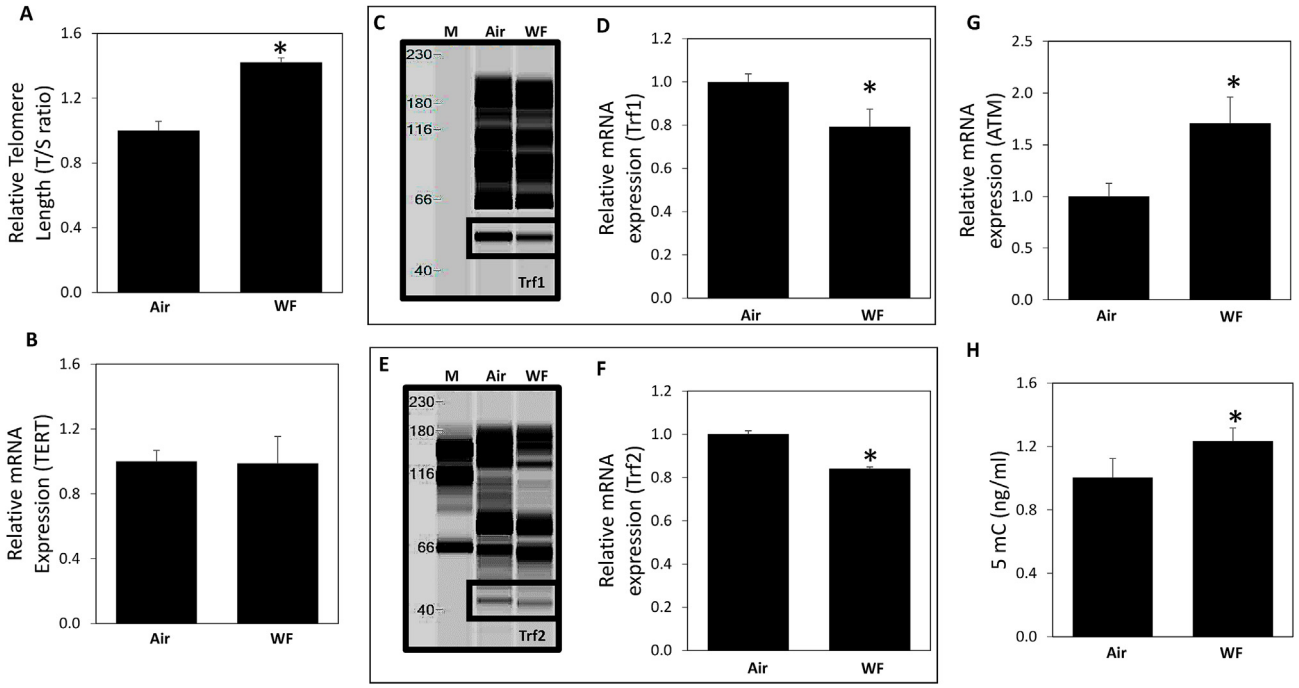

Fig. 3. (A) The relative telomere length was measured by comparing the ratio of telomere repeat copy number (T) and single gene copy number (S), expressed as T/S ratio. (B) TERT mRNA expression, (C) Trf1 mRNA expression, (D) Trf1 protein expression (~60kd), (E) Trf2 mRNA expression (F) Trf2 protein expression (~56kd), (G) ATM mRNA expression, and (H) DNA methylation was measured by assaying the production of 5-methylcytosine (5-mC) at 12 wk after WF exposure ended n#6/group; values are means ± standard error; *significantly different from air-exposed group, $p < 0.05$.

complex, Trf1 and Trf2, play an important role in telomere protection and regulation. In summary, WF inhalation may result in progressive accumulation of DNA damage in the brain, ultimately leading to the activation of ATM and eventual epigenetic modification and neurodegeneration. However, more studies are needed to evaluate the temporal effect of WF exposure on epigenetic and neurodegenerative changes, as well as, the region-specific effects in the brain.

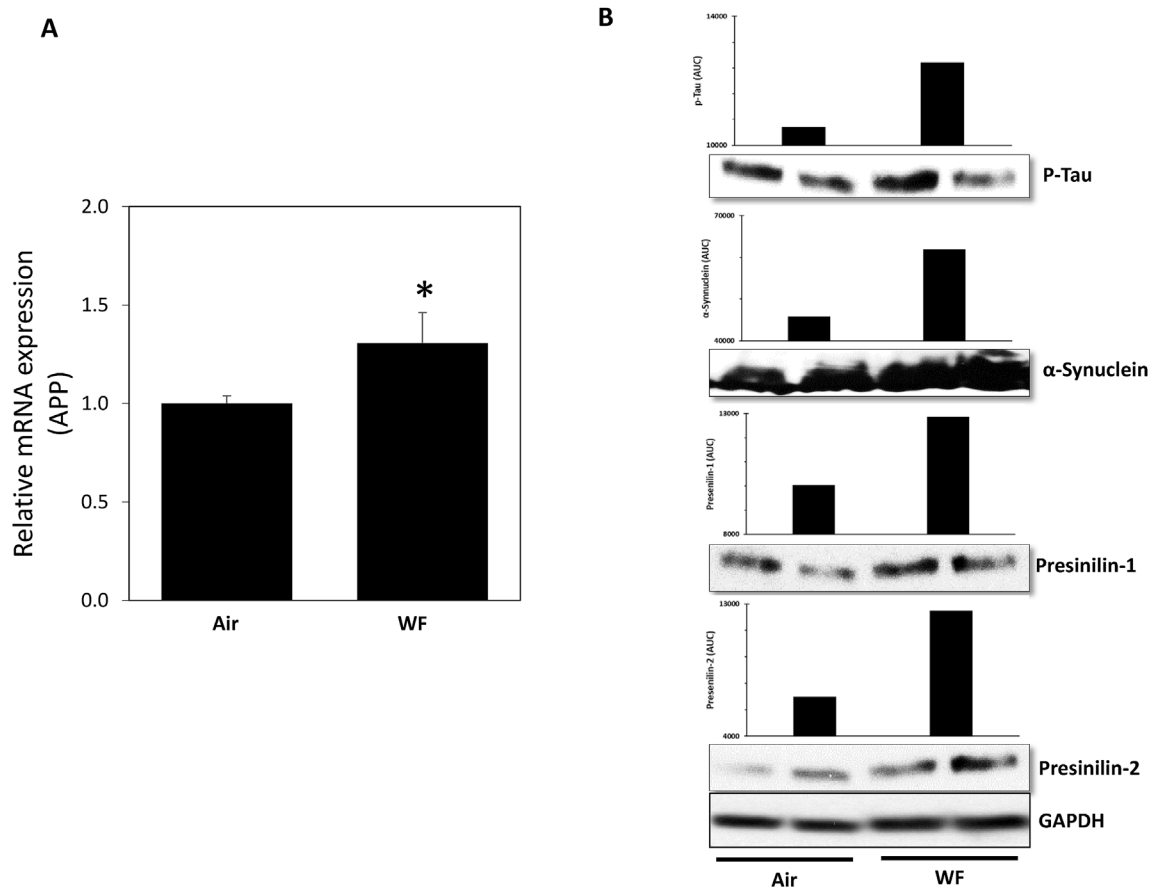

Fig. 4. (A) APP mRNA. (B) Representative Western blot and densitometer measurement of *in vivo* protein expression of p-Tau, α-synuclein, presinilin-1, presinilin-2 and GAPDH protein expression at 12 wk after WF exposure (20 mg/m^3 x 3 h/d x 4 d/wk x 5 wk). Control animals were exposed to filtered air.

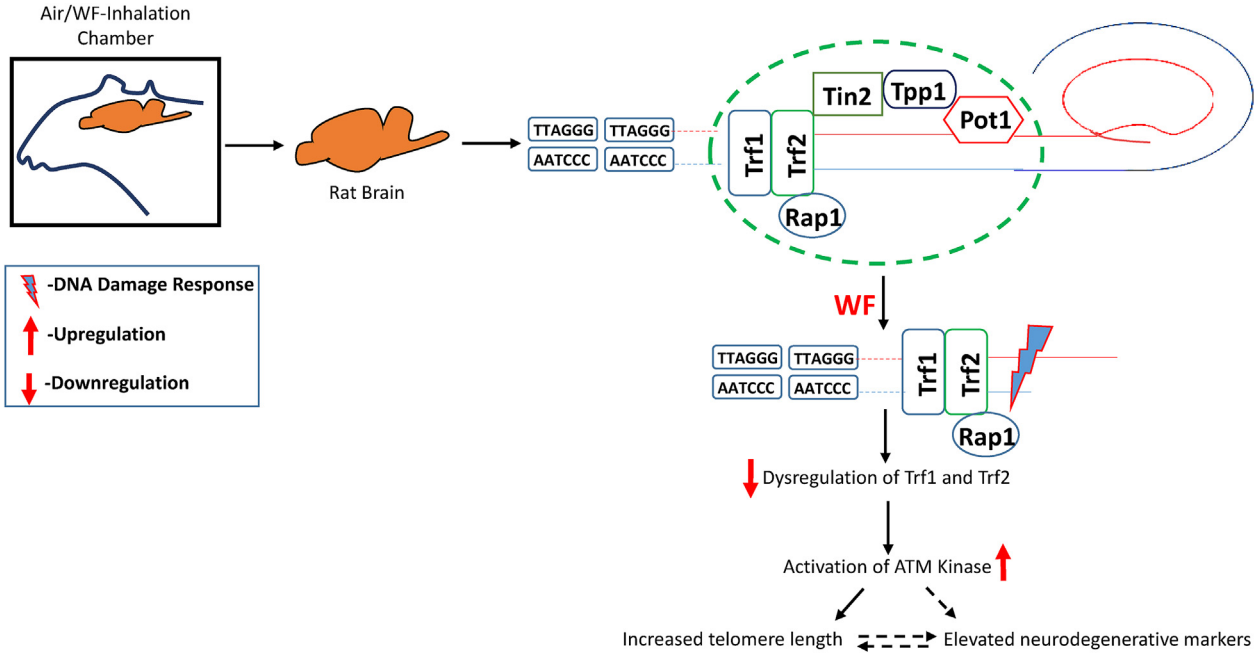

Fig. 5. Schematic diagram depicting possible association between telomere length alteration and neurodegeneration after WF inhalation through dysregulation of Trf1 and Trf2.

Disclaimer

The findings and conclusions in this report are those of the authors and do not necessarily represent the official position of the National Institute for Occupational Safety and Health, Centers for Disease Control and Prevention.

Author contributions

Exposure study design and conception: J.M.A., M.S. animal and tissue harvest: V.K., T.G.M., K.A.R., G.B., A.E., M.S. data collection, interpretation, and analysis: J.M.A., G.M.M., V.K., K.M., G.B., J.R.R., M.S. manuscript preparation and composition: J.M.A., M.S.

Declaration of competing interest

The authors declare that they have no competing interests.

Acknowledgements

This study was supported by funding from NIOSH-National Occupational research Agenda Internal Project #927ZLEG.

References

Ancelin, K., Brunori, M., Bauwens, S., Koering, C.E., Brun, C., Ricoul, M., et al., 2002. Targeting assay to study the cis functions of human telomeric proteins: evidence for inhibition of telomerase by TRF1 and for activation of telomere degradation by TRF2. Mol. Cell. Biol. 22, 3474–3487.

Antonini, J.M., Lewis, A.B., Roberts, J.R., Whaley, D.A., 2003 Apr. Pulmonary effects of welding fumes: review of worker and experimental animal studies. Am. J. Ind. Med. 43 (4), 350–360.

Antonini, J.M., Afshari, A.A., Stone, S., et al., 2006. Design, construction, and characterization of a novel robotic welding fume generator and inhalation exposure system for laboratory animals. J. Occup. Environ. Hyg. 3, 194–203.

Antonini, J.M., Roberts, J.R., Chapman, R.S., et al., 2010. Pulmonary toxicity and extrapulmonary tissue distribution of metals after repeated exposure to different welding fumes. Inhal. Toxicol. 22, 805–816.

Antonini, J.M., Roberts, J.R., Schwegler-Berry, D., Mercer, R.R., 2013 Nov. Comparative microscopic study of human and rat lungs after overexposure to welding fume. Ann. Occup. Hyg. 57 (9), 1167–1179.

Antonini, J., Kodali, V., Meighan, T., Roach, K., Roberts, J., Salmen, R., Boyce, G., Zeidler-Erdely, P., Kashon, M., Erdely, A., Shoeb, M., 2019. Effect of age, high-fat diet, and rat strain on serum biomarkers and telomere length and global DNA methylation in peripheral blood mononuclear cells. Sci. Rep. 9, 1996.

Aragon, M.J., Topper, L., Tyler, C.R., Sanchez, B., Zychowski, K., Young, T., Herbert, G., Hall, P., Erdely, A., Eye, T., Bishop, L., Saunders, S.A., Muldoon, P.P., Ottens, A.K., Campen, M.J., 2017 Mar 7. Serum-borne bioactivity caused by pulmonary multiwalled carbon nanotubes induces neuroinflammation via blood-brain barrier impairment. Proc. Natl. Acad. Sci. U. S. A. 114 (10), E1968–E1976.

Bureau of Labor Statistics, 2016. Occupational Outlook Handbook Employment:Welders, Cutter, Solders, and Brazers. U.S. Department of Labor. http://www.bls.gov/ooh, Accessed date: 14 July 2016.

Chong, L., van, S.B., Broccoli, D., Erdjument, B.H., Hanish, J., Tempst, P., de Lange, T.A., 1995. Human telomeric protein. Science 270, 1663–1667.

Compta, Y., Parkkinen, L., Kempster, P., Selikhova, M., Lashley, T., Holton, J.L., Lees, A.J., Revesz, T., 2014. The significance of α-synuclein, amyloid-β and tau pathologies in Parkinson's disease progression and related dementia. Neurodegener. Dis. 13 (2–3), 154–156. https://doi.org/10.1159/000354670. Epub 2013 Sep. 11.

Denchi, E.L., de Lange, T., 2007 Aug 30. Protection of telomeres through independent control of ATM and ATR by TRF2 and POT1. Nature 448 (7157), 1068–1071.

du Plessis, L., Laubscher, P., Jooste, J., et al., 2010. Flow cytometric analysis of the oxidative status in human peripheral blood mononuclear cells of workers exposed to welding fumes. J. Occup. Environ. Hyg. 7, 367–374.

Eriksson, P.S., Perfilieva, E., Bjork-Eriksson, T., Alborn, A.M., Nordborg, C., Peterson, D.A., Gage, F.H., 1998. Neurogenesis in the adult human hippocampus. Nat. Med. 4, 1313–1317.

Hug, N., Lingner, J., 2006. Telomere length homeostasis. Chromosoma 115, 413–425.

Kishi, S., Zhou, X.Z., Ziv, Y., Khoo, C., Hill, D.E., Shiloh, Y., Lu, K.P., 2001 Aug 3. Telomeric protein Pin2/TRF1 as an important ATM target in response to double strand DNA breaks. J. Biol. Chem. 276 (31), 29282–29291.

Kuhn, H.G., Dickinson-Anson, H., Gage, F.H., 1996. Neurogenesis in the dentate gyrus of the adult rat: age-related decrease of neuronal progenitor proliferation. J. Neurosci. 16, 2027–2033.

Kurosinski, P., Guggisberg, M., Götz, J., 2002 Jan. Alzheimer's and Parkinson's disease-overlapping or synergistic pathologies? Trends Mol. Med. 8 (1), 3–5.

Lee, E.Y., Flynn, M.R., Du, G., Lewis, M.M., Kong, L., Yanosky, J.D., Mailman, R.B., Huang, X., 2019 Apr 1. Higher Hippocampal mean diffusivity values in asymptomatic welders. Toxicol. Sci. 168 (2), 486–496.

Li, G.J., Zhang, L.L., Lu, L., Wu, P., Zheng, W., 2004 Mar. Occupational exposure to welding fume among welders: alterations of manganese, iron, zinc, copper, and lead in body fluids and the oxidative stress status. J. Occup. Environ. Med. 46 (3), 241–248.

Mamdani, F., Rollins, B., Morgan, L., Myers, R.M., Barchas, J.D., Schatzberg, A.F., Watson, S.J., Akil, H., Potkin, S.G., Bunney, W.E., Vawter, M.P., Sequeira, P.A., 2015 Sep 15. Variable telomere length across post-mortem human brain regions and specific reduction in the hippocampus of major depressive disorder. Transl. Psychiatry 5, e636.

Nera, B., Huang, H.S., Lai, T., Xu, L., 2015 Dec 7. Elevated levels of TRF2 induce telomeric ultrafine anaphase bridges and rapid telomere deletions. Nat. Commun. 6, 10132. https://doi.org/10.1038/ncomms10132.

NIOSH, 1994. Elements (ICP): method 7300. In: NIOSH Manual of Analytical Methods, fourth ed. NIOSH, Washington, DC Issue 2, U.S. Department of Health and Human Services, Publication No. 98–119.

Racette, B.A., Criswell, S.R., Lundin, J.I., Hobson, A., Seixas, N., Kotzbauer, P.T., Evanoff, B.A., Perlmutter, J.S., Zhang, J., Sheppard, L., Checkoway, H., 2012 Oct. Increased risk of parkinsonism associated with welding exposure. Neurotoxicology (Little Rock) 33 (5), 1356–1361.

Racette, B.A., Searles Nielsen, S., Criswell, S.R., Sheppard, L., Seixas, N., Warden, M.N., Checkoway, H., 2017 Jan 24. Dose-dependent progression of parkinsonism in manganese-exposed welders. Neurology 88 (4), 344–351.

Sen, S., Flynn, M.R., Du, G., Tröster, A.I., An, H., Huang, X., 2011 May. Manganese accumulation in the olfactory bulbs and other brain regions of “asymptomatic” welders. Toxicol. Sci. 121 (1), 160–167.

Shen, X., Chen, J., Li, J., Kofler, J., Herrup, K., 2016 Feb 27. Neurons in vulnerable regions of the alzheimer's disease brain display reduced ATM signaling. eNeuro 3 (1). https://doi.org/10.1523/ENEURO.0124-15.2016. pii: ENEURO.0124-15.2016.

Shoeb, M., Kodali, V.K., Farris, B.Y., et al., 2017a. Oxidative Stress, DNA methylation, and telomere length changes in peripheral blood mononuclear cells after pulmonary exposure to metal-rich welding nanoparticles. NanoImpact 5, 61–69.

Shoeb, M., Joseph, P., Kodali, V., Mustafa, G., Farris, B.Y., Umbright, C., Roberts, J.R., Erdely, A., Antonini, J.M., 2017 Dec 11b. Silica inhalation altered telomere length and gene expression of telomere regulatory proteins in lung tissue of rats. Sci. Rep. 7 (1), 17284.

Shoeb, M., Mustafa, G., Joseph, J., Umbright, C., Kodali, Roach K., Meighan, T., Roberts, J., Erdely, A., Antonini, J., 2019. Initiation of pulmonary fibrosis after silica inhalation in rats is linked with dysfunctional shelterin complex and DNA damage response. Sci. Rep. 9, 471.

Smogorzewska, A., van Steensel, B., Bianchi, A., Oelmann, S., Schaefer, M.R., Schnapp, G., et al., 2000. Control of human telomere length by TRF1 and TRF2. Mol. Cell. Biol. 20, 1659–1668.

Spallarossa, P., Altieri, P., Aloi, C., Garibaldi, S., Barisione, C., Ghigliotti, G., Fugazza, G., Barsotti, A., Brunelli, C., 2009 Dec. Doxorubicin induces senescence or apoptosis in rat neonatal cardiomyocytes by regulating the expression levels of the telomere binding factors 1 and 2. Am. J. Physiol. Heart Circ. Physiol. 297 (6), H2169–H2181.

Sriram, K., Lin, G.X., Jefferson, A.M., Roberts, J.R., Wirth, O., Hayashi, Y., Krajnak, K.M., Soukup, J.M., Ghio, A.J., Reynolds, S.H., Castranova, V., Munson, A.E., Antonini, J.M., 2010 Dec. Mitochondrial dysfunction and loss of Parkinson's disease-linked proteins contribute to neurotoxicity of manganese-containing welding fumes. FASEB J. 24 (12), 4989–5002.

Sriram, K., Lin, G.X., Jefferson, A.M., Roberts, J.R., Andrews, R.N., Kashon, M.L., Antonini, J.M., 2012 Jan 27. Manganese accumulation in nail clippings as a biomarker of welding fume exposure and neurotoxicity. Toxicology 291 (1–3), 73–82.

Thomas, P., O' Callaghan, N.J., Fenech, M., 2008 Apr. Telomere length in white blood cells, buccal cells and brain tissue and its variation with ageing and Alzheimer's disease. Mech. Ageing Dev. 129 (4), 183–190.

van der Mark, M., Vermeulen, R., Nijssen, P.C., Mulleners, W.M., Sas, A.M., van Laar, T., Huss, A., Kromhout, H., 2015 Jun. Occupational exposure to solvents, metals and welding fumes and risk of Parkinson's disease. Park. Relat. Disord. 21 (6), 635–639.

van Steensel, B., de Lange, T., 1997. Control of telomere length by the human telomeric protein TRF1. Nature 385, 740–743.

Von Zglinicki, T., 2002. Oxidative stress shortens telomeres. Trends Biochem. Sci. 27, 339–344.

Winslow, A.R., Moussaud, S., Zhu, L., Post, K.L., Dickson, D.W., Berezovska, O., McLean, P.J., 2014. Convergence of pathology in dementia with Lewy bodies and Alzheimer's disease: a role for the novel interaction of α-synuclein and presenilin 1 in disease. Brain 137, 1958–1970.

Zeidler-Erdely, P.C.1, Erdely, A., Antonini, J.M., 2012 Oct-Dec. Immunotoxicology of arc welding fume: worker and experimental animal studies. J. Immunotoxicol. 9 (4), 411–425.